The Journal of Comparative Neurology 513:98–112 (2009)

Absence of the Transcription Factor *Nfib* Delays the Formation of the Basilar Pontine and Other Mossy Fiber Nuclei

ASLI KUMBASAR,[1] CÉLINE PLACHEZ,[1] RICHARD M. GRONOSTAJSKI,[2] LINDA J. RICHARDS,[1,3] AND E. DAVID LITWACK[1]*

[1]Department of Anatomy and Neurobiology and Program in Neuroscience, University of Maryland School of Medicine, Baltimore, Maryland 21201

[2]Department of Biochemistry, Developmental Genomics Group, State University of New York and Center of Excellence in Bioinformatics and Life Sciences, Buffalo, New York 14214

[3]Queensland Brain Institute and the School of Biomedical Sciences, University of Queensland, Brisbane, Queensland, 4072, Australia

ABSTRACT

Transcription factors of the Nuclear Factor I (*Nfi*) family are important for the development of specific neuronal and glial populations in the nervous system. One such population, the neurons of the basilar pontine nuclei, expresses high levels of *Nfi* proteins, and the pontine nuclei are greatly reduced in mice lacking a functional *Nfib* gene. Pontine neurons, along with other precerebellar neurons that populate the hindbrain, arise from precursors in the lower rhombic lip and migrate anteroventrally to reach their final location. Using immunohistochemistry, we find that NFI-B expression is specific for mossy fiber populations of the precerebellar system. Analysis of the *Nfib*$^{-/-}$ hindbrain indicates that the development of the basilar pontine nuclei is delayed, with pontine neurons migrating 1–2 days later than in control animals, and that significantly fewer pontine neurons are produced. While the mossy fiber nuclei of the caudal medulla do form, they also exhibit a developmental delay. *Nfia* and *Nfix* null mice exhibit no apparent pontine phenotype, implying specificity in the action of NFI family members. Collectively, these data demonstrate that *Nfib* plays an important role in the generation of precerebellar mossy fiber neurons, and may do so at least in part by regulating neurogenesis. J. Comp. Neurol. 513:98–112, 2009. © 2008 Wiley-Liss, Inc.

Indexing terms: precerebellar; mossy fiber; cell migration; neurogenesis; hindbrain

The mature brain is composed of many subclasses of neurons and glia, each of which acquires a unique identity during development. Such identity is conferred by transcription factors that work alone or in combination to determine cell fate. One set of transcription factors that is critical for the development of specific subpopulations of both neurons and glia in the nervous system are the Nuclear Factor I (*Nfi*) transcription factors, a family consisting of *Nfia, Nfib, Nfic*, and *Nfix* (for a general review, see Gronostajski, 2000). Additional diversity in this set of factors is generated by alternative splicing, resulting in several possible isoforms for each protein. Furthermore, DNA binding and transcriptional activation require the formation of homodimers or heterodimers of different family members (Kruse and Sippel, 1994; Chaudhry et al., 1998). In vivo, *Nfi* mRNAs are expressed in overlapping but specific patterns in multiple organs throughout the body (Chaudhry et al., 1997), suggesting complex developmental roles for these transcription factors.

The role of NFI proteins in brain development is supported by several lines of evidence. First, with the exception of *Nfic*, mRNAs encoding all NFI proteins are expressed in largely overlapping yet localized patterns in the brain, placing them in a position to regulate several important developmental processes. Initially, *Nfia, Nfib*, and *Nfix* are highly expressed in ventricular zones (Chaudhry et al., 1997; Deneen et al., 2006; Plachez et al., 2008). At late embryonic and early postnatal ages, expression is particularly high in the cerebral cortex,

Grant sponsor: National Institute of Neurological Disorders and Stroke (NINDS); Grant number: NS050515-01A2 (to E.D.L.); Grant sponsor: National Health and Medical Research Council (NH&MRC, Australia); Grant number: 401616 (to L.J.R.); Grant sponsor: NH&MRC senior research fellowship (to L.J.R.).

*Correspondence to: E. David Litwack, Department of Anatomy and Neurobiology and Program in Neuroscience, University of Maryland School of Medicine, 20 Penn St., HSF2-S251, Baltimore, MD 21201.
E-mail: elitw001@umaryland.edu

Received 8 January 2008; Revised 12 September 2008; Accepted 2 November 2008

DOI 10.1002/cne.21943

Published online in Wiley InterScience (www.interscience.wiley.com).

hippocampus, basilar pontine nuclei, cerebellum, and spinal cord (Chaudhry et al., 1997; Gesemann et al., 2001; Shu et al., 2003; Deneen et al., 2006; Wang et al., 2007; Plachez et al., 2008). Second, NFI DNA binding sites are found in the promoter regions of many neuronal and glial genes, and in some cases regulate their expression (Tamura et al., 1988; Miura et al., 1990; Elder et al., 1992; Adams et al., 1995; Bedford et al., 1998; Baumeister et al., 1999; Wang et al., 2004, 2007). Third, mouse knockouts of *Nfia, Nfib*, and *Nfix* exhibit neural phenotypes in regions of the brain that express NFI genes (das Neves et al., 1999; Shu et al., 2003; Steele-Perkins et al., 2005; Campbell et al., 2008). In some cases, these defects can be linked to alterations in specific populations of cells, including both neurons and glia (Shu et al., 2003; Deneen et al., 2006; Wang et al., 2007).

We have previously found that the basilar pontine nuclei (PN) are significantly smaller in mice that lack a functional *Nfib* gene (Steele-Perkins et al., 2005). The PN is one of a number of precerebellar nuclei that provide input to, and regulate the function of, the cerebellum (Altman and Bayer, 1997). Other precerebellar nuclei include the reticulotegmental nucleus (RTN), the lateral reticular nucleus (LRN), the external cuneate nucleus (ECN), and the inferior olive (IO); the cerebellum also receives vestibular and spinal input. The role of the PN in controlling cerebellar function is illustrated by the appearance of ataxia and other motor deficits in patients with focal pontine lesions (Schmahmann et al., 2004). Therefore, understanding the development and function of the precerebellar nuclei is important for understanding motor function and sensorimotor integration.

The neurons of the precerebellar system arise from the lower rhombic lip (LRL), with partially overlapping birthdates (Taber Pierce, 1966, 1973; Altman and Bayer, 1997). Fate mapping has distinguished two lineages for precerebellar neurons, one for mossy fiber populations (PN, RTN, LRN, ECN), and one for the IO, which gives rise to climbing fibers (Rodriguez and Dymecki, 2000; Landsberg et al., 2005). Once born, precerebellar neurons move along distinct migratory routes (Bourrat and Sotelo, 1988, 1990; Altman and Bayer, 1997). Mossy fiber populations migrate over the surface of the brain. PN and RTN neurons migrate anteroventrally through the anterior extramural stream (aes), while LRN and ECN neurons migrate posteroventrally through the posterior extramural stream (pes). IO neurons also migrate ventrally and posteriorly, but they do so deep to the surface of the brain. In all cases, the ventral migration is in response to floor plate-derived netrin-1 (Yee et al., 1999; Alcantara et al., 2000) and to Slit proteins and their receptors (Causeret et al., 2002; Marillat et al., 2004; Di Meglio et al., 2008; Geisen et al., 2008). However, much remains to be answered regarding precerebellar development, including how different neuronal populations are generated from the rhombic lip, and how these subpopulations select unique pathways of migration and establish specific patterns of axonal connectivity.

The significant levels of NFI expression in the PN (Chaudhry et al., 1997; Gesemann et al., 2001) and the severe reduction of the PN in the *Nfib* mouse (Steele-Perkins et al., 2005) indicates important functions for these transcription factors in precerebellar development. Based on the pontine phenotype of the *Nfib*$^{-/-}$ mice, we have further characterized the expression of NFI-B protein in the precerebellar system using immunohistochemistry. In addition, we demonstrate here that the severe reduction of the PN previously observed (Steele-Perkins et al., 2005) is due to a delay in the development of pontine neurons, accompanied by a reduction in the production of pontine neurons. While the LRN and ECN are present, they also exhibit a developmental delay in *Nfib*$^{-/-}$ mice. These data strongly indicate that *Nfib* regulates the generation and/or migration of multiple classes of mossy fiber neurons generated from the lower rhombic lip.

MATERIALS AND METHODS

Animals

All immunohistochemistry was performed using wildtype C57BL/6J mice (Jackson Laboratory, Bar Harbor, ME) bred on-site at the University of Maryland School of Medicine animal facility. *Nfia* knockout mice, which contain a deletion of the 3′ splice acceptor site and 219 bp of the 5′ portion of exon 2 (das Neves et al., 1999), were on a C57Bl/6J background. *Nfib* knockout mice contain a genomic deletion spanning 523 bp of the 3′ portion of exon 2 and 177 bp of the 5′ portion of intron 2 (Steele-Perkins et al., 2005). These mice were backcrossed between 5 to 10 generations to a C57Bl/6J background; no differences in phenotype were observed in mice from different generations. Mice containing an *Nfix* conditional allele possessed loxP sites 406 bp upstream of and 633 bp downstream of exon 2 (Campbell et al., 2008). These mice were on a mixed 129S4/C57Bl/6J background. Mice carrying a deletion of exon 2 were created by crossing this line with an EIIa-cre transgenic mouse (Lakso et al., 1996; obtained from Jackson Laboratory). Offspring were then bred to generate *Nfix*$^{-/-}$ mice for experiments. For timed-pregnant animals, embryonic day 0 (E0) was considered the date of observation of a vaginal plug, and embryos were staged by measuring crown–rump length. All animal procedures were approved by the Institutional Animal Care and Use Committee of the University of Maryland School of Medicine.

Antibodies

Rabbit anti-NFI-B (Active Motif, Carlsbad, CA) was raised against a peptide derived from amino acids 402–415 of human NFI-B (SPQDSSPRLSTFPQ), and was used at 1:1,000 for Western blots and 1:50,000 for immunohistochemistry. The specificity of this antibody is well established (Plachez et al., 2008) and was confirmed by Western blot and immunostaining on *Nfib*$^{-/-}$ hindbrain (Fig. 1).

Rabbit anti-NFI-A (Active Motif) was raised against a peptide derived from amino acids 478–492 of human NFI-A (PSTSPANRFVSVGPR), and was used at 1:75,000 for immunohistochemistry. On Western blots of P3 mouse pontine and cerebral cortex extracts, this antibody recognized a single band of 58 kD, roughly the predicted size of the NFI-A protein (data not shown). No signal was obtained in immunostaining experiments with this antibody when blocked with immunizing peptide or on sections of *Nfia*$^{-/-}$ cerebral cortex (Plachez et al., 2008).

Rabbit anti-Pax6 raised against the 17 C-terminal residues of the mouse Pax6 protein (Davis and Reed, 1996) was obtained from Chemicon (Temecula, CA) and was used at 1:25,000 for immunohistochemistry or 1:10,000 for immunofluorescence. The staining observed using this antibody is consistent with *Pax6* mRNA localization by in situ hybridiza-

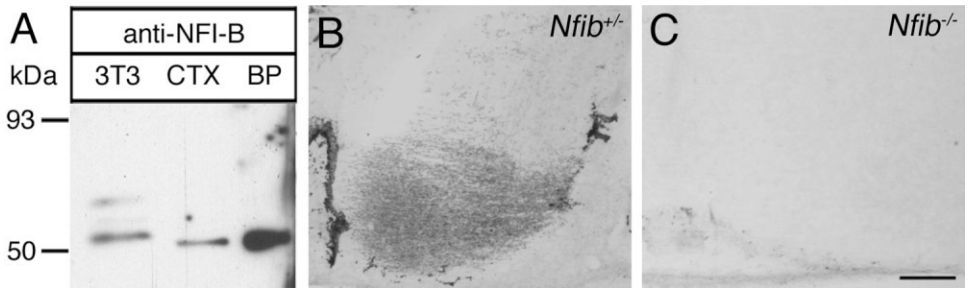

Figure 1.
Specificity of the NFI-B antibody. **A:** 20 μg of total protein from homogenates of 3T3 cells, P3 mouse cerebral cortex (CTX), and P3 basilar pontine nuclei (PN) cells were analyzed by Western blot using an anti-NFI-B antibody. Molecular weight markers in kDa are listed on the left. **B:** E17 coronal section of an *Nfib*$^{+/-}$ hindbrain immunostained for NFI-B. **C:** E17 coronal section of an *Nfib*$^{-/-}$ hindbrain immunostained for NFI-B. As demonstrated in Figures 6 and 8, some PN neurons are present in the *Nfib*$^{-/-}$ hindbrain. Nevertheless, while the PN is stained in B, no signal is observed in C. Scale bar = 200 μm in C (for B,C).

tion (Stoykova and Gruss, 1994), and with protein expression determined using other antibodies (Engelkamp et al., 1999). In addition, this antibody recognizes a band of about 50 kD on Western blots of fetal mouse brain extracts (manufacturer's technical information; also see Davis and Reed, 1996).

Rabbit anti-β-galactosidase (β-gal; Chemicon) was raised against purified β-gal from *E. coli* and was used at 1:75,000 for immunohistochemistry or 1:20,000 for immunofluorescence. Mouse anti-β-gal (Promega, Madison, WI) was used at 1:20,000 for immunofluorescence. The anti-β-gal antibody successfully stained *Nfib*$^{+/-}$ and *Nfib*$^{-/-}$ hindbrain, but did not stain *Nfib*$^{+/+}$ hindbrain (data not shown).

Mouse anti-Tag1 (4D7; Developmental Studies Hybridoma Bank, Iowa City, IA) was raised against a cell suspension prepared from embryonic cerebral cortex (Yamamoto et al., 1986) and was used at 1:1,000 for immunohistochemistry. This antibody recognizes a band of 110–135 kD by Western blot of embryonic neural tissue, consistent with the size of Tag-1 (Yamamoto et al., 1986; Dodd et al., 1988). Smaller bands of 60 kD and 80 kD have not been consistently reported. However, a 160–170 kD band has been simultaneously detected with the 135 kD protein. While this band is also detected in nonneural tissue, the 4D7 antibody does not immunostain nonneural tissue (Yamamoto et al., 1986; Dodd et al., 1988). In addition, the 4D7 antibody does not stain tissue from Tag-1 knockout mice (A. Furley, pers. commun.). Therefore, when used for immunohistochemistry this antibody does not recognize the extra species observed in Western blots. The staining of the aes and pes observed here using the 4D7 antibody is consistent with previous studies of Tag1 localization by in situ hybridization (Backer et al., 2002; Kyriakopoulou et al., 2002) and by immunostaining using a separate antibody (Wolfer et al., 1994) and this antibody (Yee et al., 1999; Kyriakopoulou et al., 2002).

Rat anti-bromodeoxyuridine (BrdU) (clone BU1/75 [ICR1]; Abcam, Cambridge, MA) was raised using BrdU as an immunogen and was used at a concentration of 1:10,000 for immunohistochemistry. No signal was obtained when this antibody was used for immunohistochemistry on tissue from mice that had not been injected with BrdU (data not shown).

For secondary antibodies, biotinylated goat antirabbit IgG (Vector Labs, Burlingame, CA), biotinylated donkey antimouse IgM, and biotinylated goat antirat IgG (Jackson Immunoresearch, West Grove, PA) were all used at 1:500. Alexa488-conjugated goat antirabbit IgG (Invitrogen, Carlsbad, CA) was used at 1:500, Alexa 488-conjugated antirat IgG (Invitrogen) was used at 1:500, and Cy3 conjugated donkey antimouse IgG was used at 1:2000–1:5000 (Jackson Immunoresearch). No secondary antibody exhibited any signal in the absence of primary antibody (data not shown).

Immunohistochemistry

Embryos from E12–E14 were immersion-fixed in 4% paraformaldehyde (PFA; prepared in phosphate-buffered saline [PBS; pH 7.4]). Embryos from E15–E18 and postnatal mice were transcardially perfused with 0.9% saline containing 1,000 U/mL heparin followed by 4% PFA and then stored in 4% PFA until use. Brains were embedded in 3% agar and sectioned at 50 μm on a Vibratome (Leica, Deerfield, IL). Floating sections were immunostained as described in Litwack et al. (2006). When detecting BrdU, sections were first treated for 45 minutes with 2N HCl, followed by a 10 minutes wash with 10 mm sodium borate, pH 8.5, and then two washes with PBS. Sections were photographed on an upright microscope (Leica) using a Phase One digital camera. For immunofluorescence, floating sections were prepared, blocked, and incubated in primary antibody as described in Litwack et al. (2006). After three washes in PBS, sections were incubated for 1–2 hours at room temperature with fluorescent conjugated secondary antibody diluted in block containing 1 μg/mL 4′,6-diamidino-2-phenylindole (DAPI) and sections were mounted on gelatin-subbed slides using PVA-DABCO. Images were collected on a laser scanning confocal microscope (Olympus) using FluoView software.

For whole-mount immunohistochemistry, brains were dissected and the meninges removed. Brains were then immersion-fixed in 4% PFA overnight at 4°C and stored in PFA until use. Immunohistochemistry on whole-mount embryos was performed as described for floating sections, except that the bleaching step was omitted and embryos were blocked for 2 hours. Photographs were taken on a Nikon stereomicroscope using ACT-1 software.

Brightness and contrast of scanned images were adjusted using Adobe Photoshop CS (San Jose, CA). Stained sections were compared with those illustrated in Jacobowitz and Ab-

bott (1998) and Paxinos and Franklin (2001) for identification of neuroanatomical regions.

In situ hybridization

Tissue fixed in 4% PFA was cryoprotected in 30% sucrose and 20 μm cryostat sections were collected on Superfrost Plus slides (Fisher, Pittsburgh, PA). Sections were fixed for 15 minutes in 4% PFA in PBS, washed three times in PBS, treated with 3 μg/mL proteinase K (Roche, Nutley, NJ) for 3 minutes, postfixed for 15 minutes in 4% PFA washed three times in PBS, acetylated for 10 minutes in 0.25% acetic anhydride in 0.1 M triethanolamine, and washed three times in PBS. Sections were then prehybridized for 1 hour in hybridization solution (50% deionized formamide, 5× SSC [pH 4.5], 1% SDS, 50 μg/mL yeast tRNA, 50 μg/mL heparin), and then incubated at 70°C overnight with ≈0.3 μg/mL DIG-labeled *Barhl1* probe (corresponding to nucleotides 1–1593 of Access. No. AJ237590; Li et al., 2004) in hybridization solution. The following day, sections were washed three times for 15 minutes each in 50% formamide, 2× SSC, 1% SDS at 70°C, and three times in TBST (25 mM Tris [pH 7.5], 136 mM NaCl, 2.68 mM KCl, 1% Tween-20) at room temperature. Sections were then incubated for 1 hour in blocking buffer (1.5% Blocking Reagent [Roche], 100 mM Tris [pH 7.5], 0.15 M NaCl), and then overnight at 4°C in 1:5000 alkaline phosphatase-conjugated anti-digoxigenin antibody (Roche). Sections were then washed three times in TBST, twice in NTMT (100 mM Tris [pH 9.5], 100 mM NaCl, 50 mM $MgCl_2$), and then developed several hours to overnight in BM Purple (Roche).

In situ hybridization on whole-mount preparations of mouse hindbrain using an *Nfix* antisense RNA probe corresponding to nucleotides 964–1185 of Access. No. U57636 (Chaudhry et al., 1997) was performed as described in Yee et al. (1999).

Counting of BrdU- and β-gal-positive cells

Timed-pregnant E13 mice received an intraperitoneal injection of bromodeoxyuridine (BrdU; 70 μg/g; Sigma, St. Louis, MO). Embryos from injected mice were transcardially perfused with 4% PFA at E18. The 50 μm coronal sections were taken through the entire PN using a vibratome and then immunostained for BrdU and β-gal as described above. Cell counts were determined using unbiased optical dissector methodologies (Howard and Reed, 2005). For each brain the PN on every third section (with a random section rostral to the PN selected as the starting point) was imaged by confocal microscopy. Random fields (four 60× objective fields per section) were collected for $Nfib^{+/-}$ and $Nfib^{-/-}$ mice (in the latter case, the entire BP was imaged due to its significantly smaller size, with some cases requiring fewer that four fields). A z-series composed of optical sections spaced at 5 μm was collected for each random field. Within each image stack, BrdU+ cells were counted in 10 random 20 × 20 μm dissectors using the Neurolucida software package (MicroBrightField, Williston, VT); BrdU+ cells were only counted if they coexpressed β-gal and were contained within or intersected with the upper or left border of the dissector. A separate set of counts was performed to estimate β-gal+ cells; these were counted from five random 20 × 20 μm dissectors. Cell density (N_V) was calculated using the following formula: $N_V = Q/V_{dis}$, where Q is the total number of cells counted, and V_{dis} is the total volume of the dissectors used for counting. The volume of the PN (V) was calculated using the Cavalieri method (Howard and Reed, 2005) after measuring the area of the β-gal+ domain in every third section. The total number of counted cells in the PN (N) was estimated as $N = N_V \times V$. Comparisons of N between genotypes were made by unpaired *t*-test using Prism software (GraphPad Software, La Jolla, CA).

Western blot analysis

Extracts of 3T3 cells were prepared by boiling monolayers directly in 50 mM Tris (pH 7.4), 1% SDS with protease inhibitors (3 mM EDTA, 10 μg/mL pepstatin A, 5 μg/mL leupeptin, 1 mM phenylmethylsulfonyl fluoride [PMSF]). After centrifugation for 10 minutes the supernatant was saved for analysis. Cerebral cortical and PN extracts were prepared by homogenizing tissue in 1% Triton X-100, 25 mM Hepes (pH 7.5), 0.15 M NaCl with protease inhibitors. Extracts were analyzed by Western blotting as described in Litwack et al. (2004).

RESULTS

We have previously reported that the PN appears severely reduced in $Nfib^{-/-}$ mice (Steele-Perkins et al., 2005). To begin to understand the basis for this phenotype, we further characterized the expression of *Nfib* during development of the precerebellar nuclei of the hindbrain. Past studies have used in situ hybridization to demonstrate the expression of *Nfib* mRNA in the PN (Chaudhry et al., 1997; Gesemann et al., 2001). To determine if NFI-B protein is expressed in the PN and to further characterize the specificity of the NFI-B antibody for hindbrain tissue, we performed Western blots on extracts of P3 mouse PN and cerebral cortex using an antibody raised against an NFI-B-derived peptide. A single 63 kD band was detected in both pontine and cortical extracts (Fig. 1A), consistent with the predicted molecular weight of NFI-B. In 3T3 cell extracts, two slightly larger bands were observed, suggesting either that neural tissue expresses an alternatively spliced isoform of NFI-B, or that there are differences in post-translational modifications of NFI-B between 3T3 cells and brain. The bands detected here represent NFI-B, as this antibody does not crossreact with other NFI family members on Western blots (Plachez et al., 2008). In addition, while the NFI-B antibody stains the cerebral cortex and PN in control animals, it does not stain either structure in $Nfib^{-/-}$ animals (Fig. 1B,C; and Plachez et al., 2008). Below, we use this antibody to examine the distribution of NFI-B protein in the LRL, and during the migration of precerebellar neurons and the appearance of the precerebellar nuclei.

NFI-B is expressed in the lower rhombic lip

The precerebellar nuclei (PN, RTN, LRN, ECN, and IO) all derive from the precerebellar neuroepithelium of the LRL, which is located along the fourth ventricle between the alar plate and the roof plate. At E12, when LRN and ECN neurons are being generated and pontine neurogenesis is commencing, NFI-B expression was observed in the LRL, with lower but significant expression levels in the rest of the ventricular zone aligning the fourth ventricle (Fig. 2A). Expression in the LRL is maintained at E14 and at E16 (Figs. 2B, 3A, 4D).

The entire precerebellar rhombic lip expresses Pax6 (Engelkamp et al., 1999; Landsberg et al., 2005), and two subdomains can be delineated by staining for specific markers. The first is a dorsal Math1-positive subdomain that gives rise to

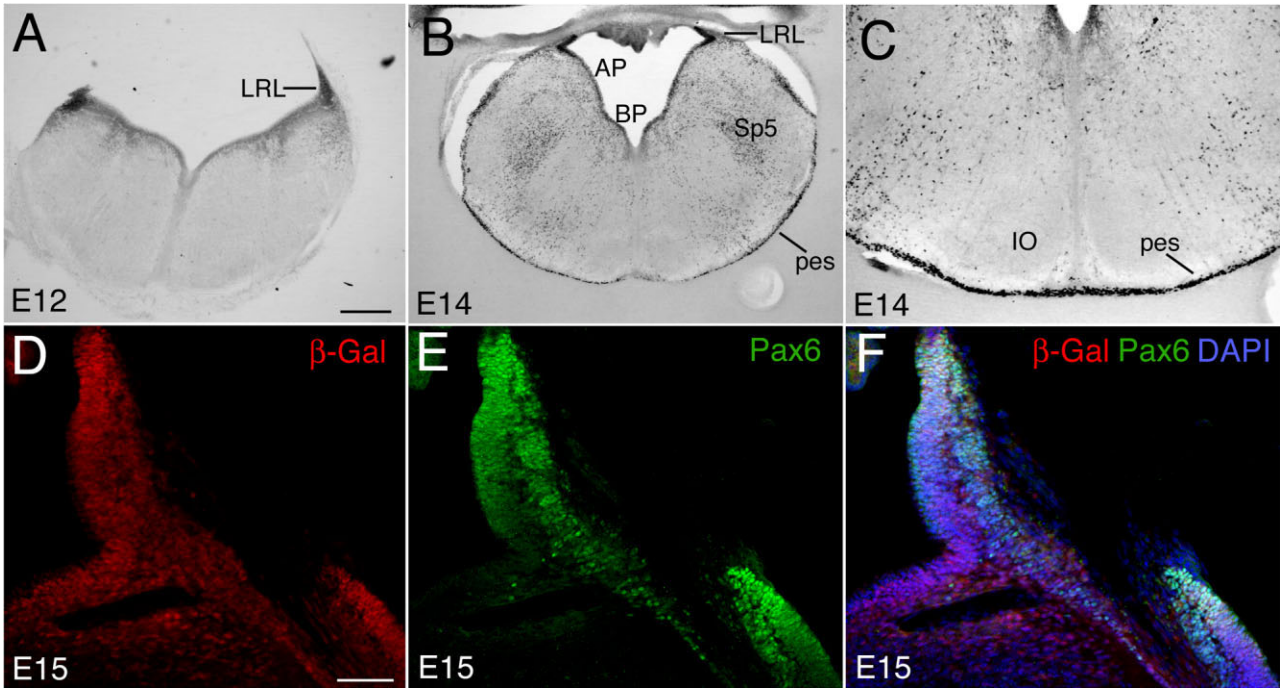

Figure 2.
NFI-B expression in the E12–E15 hindbrain. **A–C:** NFI-B immunohistochemistry on coronal sections of (A) E12 and (B,C) E14 hindbrain. C is a higher magnification view of a section similar to that shown in B. The lower rhombic lip (LRL) expresses the highest NFI-B levels at both ages, with expression also observed in the alar plate (AP) and basal plate (BP), and, by E14, in the posterior extramural stream (pes). Expression in the spinal trigeminal nucleus (Sp5) is also seen. The inferior olive (IO) does not express NFI-B. **D–F:** Double immunostaining for (D) β-gal and (E) Pax6 on a coronal section E15 *Nfib*$^{+/-}$ hindbrain. F shows an overlay of β-gal (red) and Pax6 (green), along with DAPI staining (blue). Scale bars = 200 μm in A (for A,B); 100 μm in D (for C–F).

mossy fiber neurons, and the second is a ventral Neurogenin-1-positive subdomain that gives rise to climbing fiber neurons (Landsberg et al., 2005). To determine if NFI-B expression in the LRL is specific to either of these subdomains, we took advantage of mice in which most of exon 2 of the *Nfib* gene has been replaced with a *lacZ* reporter gene (Steele-Perkins et al., 2005). *Nfib*$^{+/-}$ mice have a phenotypically normal PN (see below), and double staining experiments indicate that 92% of cells in the aes (n = 113 total cells counted) and 97% of the cells in the PN (n = 102 total cells counted) express both NFI-B and β-gal (data not shown). Furthermore, the distribution of NFI-B and β-gal in the developing PN are identical (for E14, compare NFI-B staining in Fig. 3A,B to β-gal staining in Fig. 6A,B; for E16, compare NFI-B staining in Fig. 4A to β-gal staining in Fig. 6D). Staining of *Nfib*$^{+/-}$ mice for both β-gal (Fig. 2D) and Pax6 (Fig. 2E) demonstrates that in the LRL the Pax6 domain is contained entirely within the NFI-B domain, the latter of which extends throughout the entire ventricular zone along the fourth ventricle. We therefore conclude that NFI-B expression is not limited to any particular subdomain of the LRL.

Expression in precerebellar mossy fiber nuclei of the caudal medulla

Despite their apparently common origin in the rhombic lip, the neurons that comprise the precerebellar nuclei take different migratory routes through the developing hindbrain (Altman and Bayer, 1997). At E14, LRN and ECN neurons, which are migrating through the caudal medulla via the posterior extramural stream (pes), express significant levels of NFI-B (Figs. 2B,C, 3C,F). In whole-mount preparations of E14 hindbrain, NFI-B expression coincides with that of Tag1 (Fig. 3D), a cell adhesion molecule expressed in the pes at this age (Wolfer et al., 1994; Backer et al., 2002; Kyriakopoulou et al., 2002). We were unable, however, to visualize the intramural pathway taken by migrating IO neurons using NFI-B immunostaining, and the IO itself does not express NFI-B (Figs. 2C, 5E).

By E16, the migration of LRN and ECN neurons is nearing completion. NFI-B expression at E16 persists in cells populating the pes (Fig. 4A,C,D); on the dorsal surface, the pes appears to arise from the same location as does the aes (Fig. 4D). Consistent with observations reported by Kyriakopoulou et al. (2002), we do not observe Tag1 in the pes at this age (Fig. 4B). Therefore, the cells in the E16 pes likely represent a late-migrating population of precerebellar neurons, although we cannot rule out that these could be a mature population of NFI-B+ cells residing on the surface of the caudal medulla. At P0, NFI-B is expressed in the LRN and ECN, but not in the IO (Fig. 5E), consistent with observations made at earlier embryonic ages.

NFI-B expression in the developing PN

By E14 the first PN neurons have left the LRL and are en route to the ventral surface of the hindbrain via the aes. In whole-mount preparations we found that NFI-B is expressed in the E14 aes. In particular, labeled cells can be seen depart-

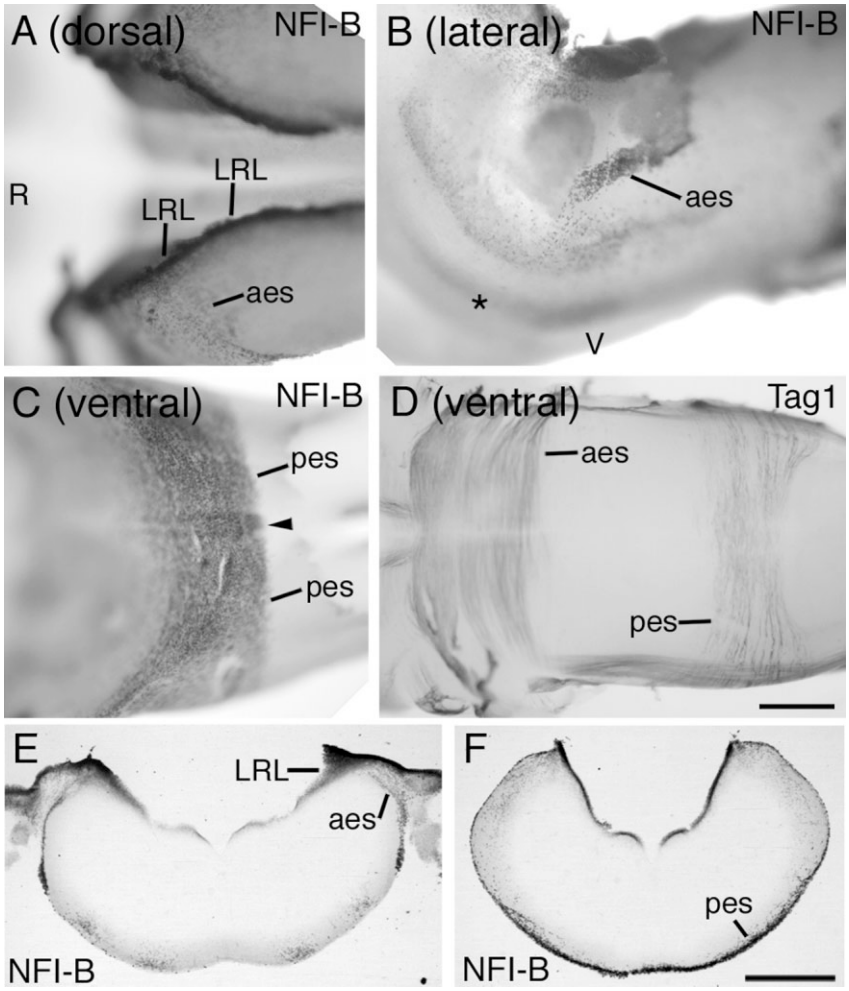

Figure 3.
NFI-B expression in migrating precerebellar neurons at E14. Whole-mount preparations of E14 hindbrain were immunostained for NFI-B (A–C,E,F) or Tag1 (D). Rostral (R) is to the left in A–D, and ventral (V) is down in B. **A:** Dorsal view of the hindbrain, stained for NFI-B, shows expression in the LRL and in aes after it has emerged from the LRL. **B:** Lateral view of the same brain as in A, showing NFI-B expression in the aes. Migrating PN neurons have not yet reached the ventral surface of the hindbrain (asterisk). **C:** Ventral view of the caudal medulla of the same brain as in A, showing NFI-B expression in the pes. Arrowhead indicates the ventral midline. **D:** Tag1 immunostaining of an E14 hindbrain, showing the positions of the aes and the pes. **E,F:** Rostral and caudal coronal sections of the brain in A, confirming expression in the LRL, aes, and pes. Deeper structures are not stained due to the limited penetration of the antibody in whole-mount experiments. Scale bars = 350 μm in D (for A–C); 500 μm (for D); 0.5 mm in E (for E,F).

ing the LRL; however, no labeled cells can yet be seen on the ventral surface of the hindbrain (Fig. 3A,B). The localization of NFI-B to the E14 aes overlaps with Tag1 (Fig. 3D), which is expressed in fibers associated with migrating PN neurons (Wolfer et al., 1994; Yee et al., 1999). Cross-sections of immunostained whole mounts confirm that labeled cells in both the aes and pes lie on the surface (Fig. 3E,F).

At E16, PN neuron migration has reached its peak, with noticeable nuclei forming adjacent to the ventral midline. Consistent with this timing, significant NFI-B expression is observed in the E16 aes (Fig. 4A,C,D). In particular, NFI-B+ cells are distributed in a discrete stream from the dorsal surface of the hindbrain to the ventral midline, coursing around the trigeminal nerve en route, and are also apparent in the PN itself. This expression is again similar to that of Tag1 (Fig. 4B). NFI-B is also expressed in cells directly overlying the ventral midline (Fig. 4A), and may represent an early population of migrating pontine neurons that cross the midline (Kawauchi et al., 2006; Okada et al., 2007).

NFI-B is expressed in the late embryonic and early postnatal PN, and then is gradually downregulated during maturation. We observed NFI-B in both the PN and the RTN at E18 and P0 (Fig. 5A–C). By P0, the PN is still positive for NFI-B, which, while relatively uniform, exhibits a small dorsal domain of high expression (Fig. 5C). At P7, NFI-B is still found in the PN, but in an even more patchy distribution with high levels concentrated dorsomedially (Fig. 5D). No significant levels of NFI-B are observed in the adult (Fig. 5F).

Pontine development is delayed in *Nfib*-deficient mice

To determine the nature of the PN phenotype observed in *Nfib*$^{-/-}$ mice, we used immunohistochemistry for β-gal to

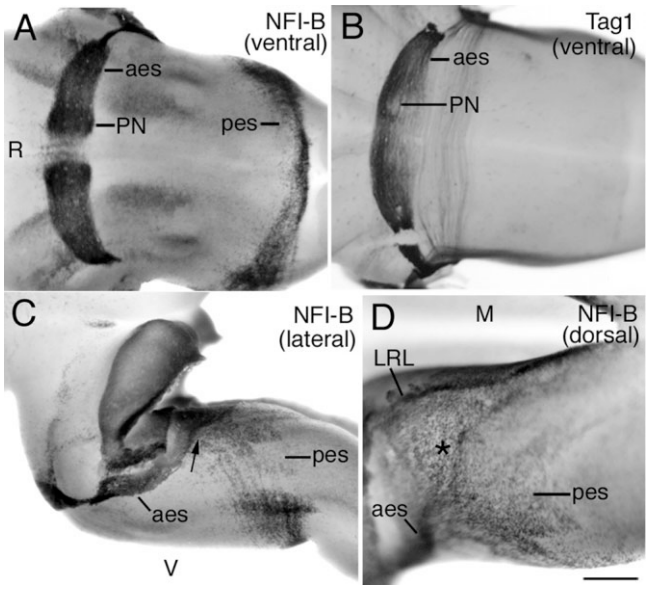

Figure 4.
NFI expression in migrating precerebellar neurons at E16. Whole-mount preparations of E16 hindbrain were immunostained for NFI-B (A,C,D) or Tag1 (B). Rostral (R) is to the left in A–D, ventral (V) is down in C, and medial (M) is up in D. **A:** Ventral view of hindbrain immunostained for NFI-B, showing expression in the aes, pes, and PN. **B:** Ventral view of hindbrain immunostained for Tag1, showing expression in the aes and PN but not in the caudal medulla. **C:** Lateral view of the same brain as in A, showing NFI-B expression in the LRL, aes, and pes. Note that the aes and pes appear to originate from the same region (arrow) proximal to the LRL. **D:** Dorsal view of the same brain as in A, demonstrating NFI-B expression in the LRL, aes, and pes. As in C, note that the pes originates from the same region as the aes (asterisk). Scale bar = 500 μm in D (for A–C); 300 μm for D.

follow the fate of NFI-B-expressing cells in *Nfib*$^{+/-}$ and *Nfib*$^{-/-}$ hindbrain. Dorsolateral views of E14 whole mounts show the β-gal+ cells of the *Nfib*$^{+/-}$ and *Nfib* $^{-/-}$ aes and pes (Fig. 6A,A'). The aes of *Nfib*$^{-/-}$ mice is visibly reduced compared to that of *Nfib*$^{+/-}$ mice (Fig. 6A,A',B,B'). In addition, no β-gal+ cells are observed on the ventral surface of *Nfib*$^{-/-}$ hindbrain, where at this age the first migrating PN neurons are normally at or near the midline (Fig. 6B,B'). Similar results, notably an absence of β-gal+ cells in the ventrolateral hindbrain, were observed in immunostained coronal E14 sections (Fig. 8A,A'). These results demonstrate that, although the *Nfib*$^{-/-}$ aes is forming at E14, it is smaller and has not extended as far as in control animals. This suggests that the formation of the aes and the PN might be delayed in *Nfib*$^{-/-}$ mice.

Analysis of hindbrains at E15–E18 is consistent with a delay in PN development, as the morphology of the aes and the PN in *Nfib*$^{-/-}$ mice consistently appears similar to that of controls that are 1–2 days younger. At E15, *Nfib*$^{+/-}$ pontine migratory neurons have arrived at and are distributed across the ventral midline (Fig. 6C), consistent with observations of an early population of crossing PN neurons (Kawauchi et al., 2006; Okada et al., 2007). In *Nfib*$^{-/-}$ mice, however, the aes does not extend to the midline; instead, the first β-gal+ cells have just appeared on the ventral surface (Fig. 6C', labeled aes). At E16, *Nfib*$^{+/-}$ PN neuron migration has reached its peak and discernible β-gal+ nuclei are starting to form adjacent to the midline (Fig. 6D). Immunostaining of coronal sections indicate that some β-gal+ cells have entered the hindbrain parenchyma (data not shown). In E16 *Nfib*$^{-/-}$ hindbrains, β-gal+ cells in the aes have reached the midline and are distributed across it (Fig. 6D'); however, the size of the aes appears smaller, and no obvious PN can be identified (compare Fig. 6C and 6D'). Analysis of staining in coronal sections confirms that the aes is present, albeit reduced in E16 *Nfib*$^{-/-}$ hindbrains, and also demonstrates that no β-gal+ cells have entered the parenchyma (data not shown). At E17 and E18, the PN is clearly observed in *Nfib*$^{+/-}$ animals, with the aes having an increasingly "streaky" appearance consistent with a decrease in the number of migrating PN neurons (Fig. 6E,F). In *Nfib*$^{-/-}$ mice at these ages, the aes is more prominent, appearing more similar to control aes at E16; in addition, smaller but discernable PN are observed, and some β-gal+ cells are still distributed over the midline (Fig. 6E',F'). Overall, in *Nfib*$^{-/-}$ mice, pontine development lags that in control animals by $\approx$1.5–2 days (Steele-Perkins et al., 2005). Analysis of postnatal PN formation at later ages was not possible due to the perinatal lethality of *Nfib*$^{-/-}$ mice. Therefore, while the mutant PN is clearly smaller than controls at E18, it is unclear whether, given sufficient time, the mutant PN would eventually reach a near-normal size.

As Pax6 is expressed in migrating precerebellar neurons (Engelkamp et al., 1999), we used it to confirm and extend the observations of PN neuron development made using immunostaining for β-gal. By double labeling for both β-gal and Pax6, we find that 65% of β-gal+ cells in the aes also express Pax6 (n = 122 total cells counted), with the remainder singly labeled for β-gal (Fig. 7A–C,A'–C'). Therefore, Pax6 is expressed in a subset of NFI-B-expressing cells, a finding consistent with a previous observation that Pax6 is not expressed in all migrating PN neurons (Schmid et al., 2007). However, it is possible that Pax6 levels are too low in some cells to be detected using our immunostaining protocol. Nevertheless, the overall distribution of β-gal and Pax6 was identical within the aes. In addition, whereas the *Nfib*$^{+/-}$ aes at E15 has reached the ventral midline, staining of E15 *Nfib*$^{-/-}$ hindbrain for Pax6 and for β-gal revealed a thinner aes that had only progressed as far as the revealed hindbrain (Fig. 7D–F,D'–F').

A time course of Pax6 expression in coronal hindbrain sections revealed a delay consistent with that observed using whole-mount β-gal staining. At E14 the aes is visible in the ventral hindbrains of control but not *Nfib*$^{-/-}$ mice (Fig. 8A,A'). In addition, similar to observations made in β-gal-stained whole mounts (Fig. 6A,B), the aes more proximal to the LRL was observed in both control and *Nfib*$^{-/-}$ animals, although it was smaller in the latter (Fig. 8B,B'). In E16 control animals, Pax6+ cells are just lateral to the ventral midline, and have entered the hindbrain parenchyma to form the PN (Fig. 8C). In E16 *Nfib*$^{-/-}$ mice these cells were only observed lateral to the region of the PN (Fig. 8C). By E18, the PN of control animals is well formed and the aes has thinned (Fig. 8D). In comparison, while Pax6+ cells in *Nfib*$^{-/-}$ hindbrain have clearly entered the hindbrain parenchyma at the correct location, the PN is significantly smaller (Fig. 8D'). At the same time, the aes appears larger than in control hindbrain, suggesting that more PN neurons are migrating in the knockout at this age. Similar results were obtained in coronal sections stained for β-gal

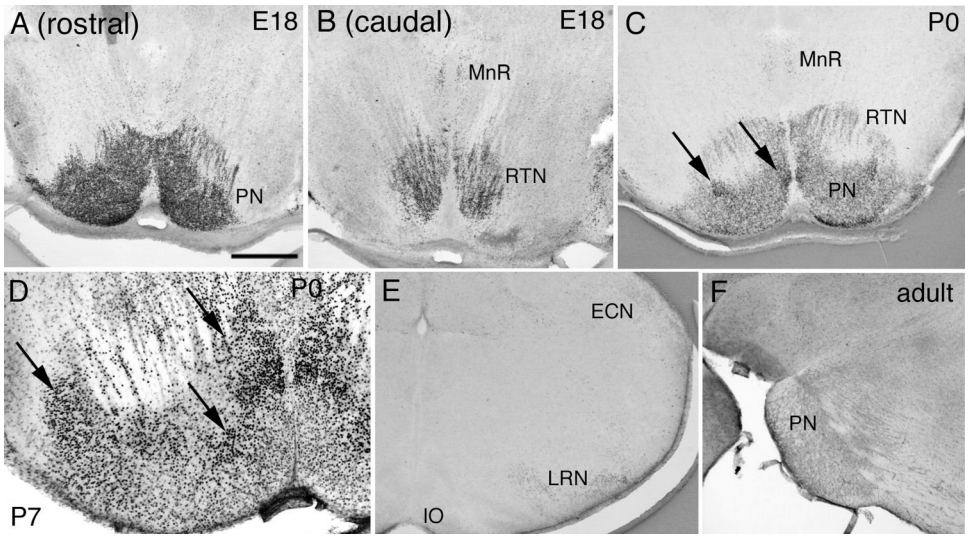

Figure 5.
NFI-B expression in the postnatal precerebellar nuclei. **A,B:** Rostral and caudal coronal sections, respectively, through the E18 PN, showing expression in the PN, the reticulotegmental nuclei (RTN), and the median raphe (MnR). **C:** Coronal section of P0 pons stained for NFI-B. Arrows indicate PN subdomains with higher levels of NFI-B expression. **D:** Coronal section of P7 hindbrain stained for NFI-B. Arrows indicate PN subdomains with higher levels of NFI-B expression. **E:** Staining of P0 caudal medulla for NFI-B. Expression is observed in the LRN and external cuneate nucleus (ECN). No expression is observed in the IO. **F:** Sagittal section of adult hindbrain stained for NFI-B. Little if any NFI-B expression is seen in the PN at this age. Scale bar = 500 μm in A (for A–C,E); 250 μm for D; 400 μm for F.

(data not shown). In general, the use of Pax6 as a marker of migrating neurons confirms the delay in PN formation initially observed by β-gal immunostaining.

BrdU birthdating in *Nfib*-deficient mice suggests a reduction of pontine neurogenesis at E13

Visual inspection of the *Nfib*$^{-/-}$ PN suggested that it is generally smaller. A count of β-gal+ cells at E18 indicated that there was an ≈90% reduction in cell number in the *Nfib*$^{-/-}$ PN (*Nfib*$^{+/-}$: 85,815 ± 4,075, n = 3; *Nfib*$^{-/-}$: 9,598 ± 666, n = 3; $P < 0.001$) (Fig. 9). While this could result from normal but delayed production of pontine neurons, it may also be that fewer pontine neurons are generated. To assess this, we injected timed-pregnant mice at E13 with BrdU, and analyzed the number of BrdU+ cells in the PN at E18 (Fig. 9). Pontine neurogenesis is commencing at E13 and, as expected, more BrdU+ cells were found dorsally and centrally within the PN in both samples; these cells correspond to the normal location of the earliest born pontine neurons (Altman and Bayer, 1997). As with β-gal, there was an ≈90% reduction in BrdU+ cells in the *Nfib*$^{-/-}$ PN (*Nfib*$^{+/-}$: 4,699 ± 1,421, n = 3; *Nfib*$^{-/-}$: 340 ± 30, n = 3; $P < 0.05$). These results suggest that, in the absence of *Nfib,* neurogenesis is aberrant at a time when the first pontine neurons are normally born.

Precerebellar mossy fiber neurons of the caudal medulla exhibit a developmental delay in the absence of *Nfib*

Like the PN, the LRN and ECN also express NFI-B throughout their development. We therefore determined if loss of *Nfib* also affects the development of these nuclei. In contrast to the large reduction of the PN, the LRN and ECN are easily identifiable in E18 *Nfib*$^{-/-}$ hindbrain by in situ hybridization for *Barhl1*, a marker of mossy fiber nuclei (Fig. 10). While the ECN appears grossly normal, the LRN is expanded toward the ventral midline, and at some levels of the caudal medulla ectopic *Barhl1* expression is observed at the midline, in the region of the inferior olive (arrowhead in Fig. 10D). This ectopic expression is not confined to the surface of the hindbrain, but instead extends into the parenchyma along the medial side of the inferior olive.

Analysis of LRN development in *Nfib*$^{-/-}$ mice reveals a delay in the development of the pes. At E13, *Barhl1* expression is observed in the pes, and stretches down to the ventral midline (Fig. 11A). In the *Nfib*$^{-/-}$ hindbrain, however, *Barhl1* expression is only found just outside the rhombic lip (Fig. 11A'), suggesting that the precerebellar neurons of the caudal medulla have been generated but have not migrated as far as normal. At E14 and E15, whole-mount immunohistochemistry for β-gal demonstrates the presence of a well-developed pes in both control and mutant hindbrains (Fig. 11B,B',C,C'). At these ages, β-gal+ cells are distributed across the midline, which is consistent with the normal crossing of migrating LRN and ECN neurons. By E16 and later, control hindbrains exhibit a reduction in labeled cells at the midline, while the LRN itself becomes apparent (Fig. 11D–F). In *Nfib*$^{-/-}$ whole mounts at E16, however, there are still many more labeled cells at the midline, and the LRN cannot yet be distinguished as a discrete nucleus (Fig. 11D'). While the LRN becomes apparent in mutants by E17, labeled cells remain at the midline as late as E18 (Fig. 11E',F'), consistent with the ectopic Barhl1 expression observed in Figure 9D. In total, although the LRN and ECN form, these data indicate a delay in the development of the caudal precerebellar nuclei. In addition, the presence of ectopic cells near the ventral midline suggests that some cells may either be misspecified or have targeted the incorrect site during migration.

Formation of the PN is unaffected in *Nfia* and *Nfix* null mice

In addition to NFI-B, we find that NFI-A and NFI-X are expressed in both the aes and the PN (Fig. 12A,B), in agreement with previous studies of NFI distribution in the brain (Chaudhry et al., 1997; Gesemann et al., 2001). However, defects of PN development have not been reported in *Nfia*$^{-/-}$ and *Nfix*$^{-/-}$ mice. To examine PN development in these animals, we performed Pax6 immunostaining on E18 *Nfia*$^{-/-}$ and *Nfix*$^{-/-}$ hindbrain. In *Nfia*$^{+/+}$ and *Nfix*$^{+/+}$ mice, the PN were clearly visible and the aes was detected as a thin stream of Pax6+ cells (Fig. 12C,E). In *Nfia*$^{-/-}$ and *Nfix*$^{-/-}$ hindbrains, the PN and aes were also clearly visible (Fig. 12D,F), with no significant difference in its size when compared to control hindbrain. Thus, at a gross level the formation of PN appears unaffected in *Nfia* and *Nfix* null mice.

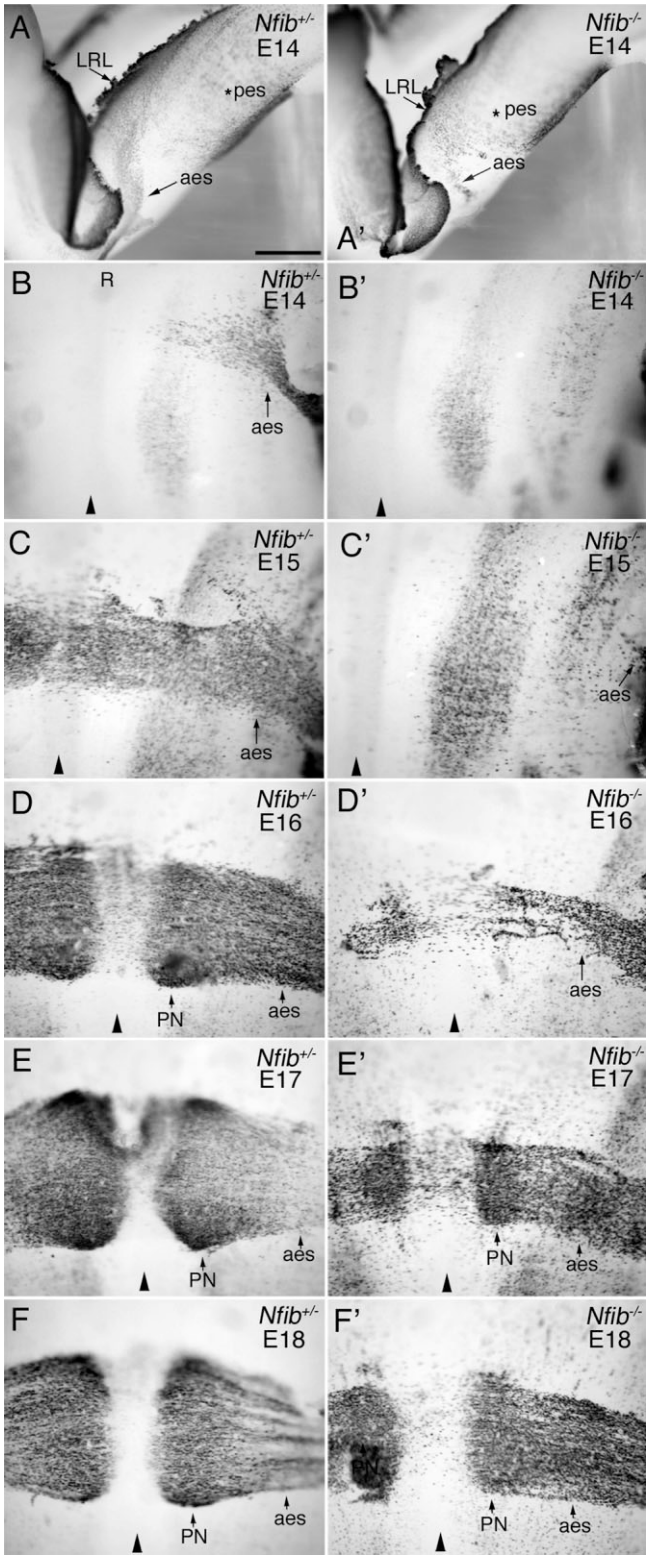

DISCUSSION

Members of the NFI family of transcription factors are critical for the development of the nervous system. Previous studies have found that *Nfib* mRNA is expressed at high levels in the developing PN (Chaudhry et al., 1997), and that the PN is greatly reduced in the absence of *Nfib* (Steele-Perkins et al., 2005). Based on these observations, we examined the pattern of NFI-B protein expression during brainstem development and found that mossy fiber neurons of the precerebellar system express NFI-B. In addition, analysis of *Nfib*$^{-/-}$ mice indicates that the PN phenotype is due to a developmental delay, and that such a delay is also observed in the mossy fiber neurons of the caudal medulla. Such delays may indicate a function for NFI-B in one or more processes that regulate neuronal development, including neurogenesis and cell migration.

NFI-B expression in the precerebellar system

Pontine neurons, like those of the other precerebellar nuclei, are derived from the LRL. In particular, the mossy fiber precerebellar nuclei emerge from a specialized Math1-positive compartment within the LRL (Landsberg et al., 2005; Machold and Fishell, 2005; Wang et al., 2005) and migrate along the surface of the brain to reach their final destinations. Our results using an antibody specific to NFI-B are consistent with previous findings of *Nfib* mRNA expression in the PN and in migrating pontine neurons (Chaudhry et al., 1997). In addition, we have found that NFI-B is expressed in the mossy fiber nuclei of the caudal medulla, but not in the inferior olive, which is composed of climbing fiber neurons. This pattern of expression fits with the observation that NFI-B and other NFI factors are expressed in cerebellar granule neurons (Wang et al., 2007), which are developmentally similar to precerebellar neurons in that they derive from the upper rhombic lip and ex-

Figure 6.
Analysis of β-gal expression in *Nfib*$^{-/-}$ hindbrains indicates a delay in PN development. Whole-mount preparations of E14–E18 **(A–F)** *Nfib*$^{+/-}$ and **(A'–F')** *Nfib*$^{-/-}$ hindbrains were immunostained for β-gal. A,A': Dorsolateral view (rostral is to the left) of β-gal expression in E14 hindbrains shows precerebellar neurons originating from the LRL and migrating circumferentially. Note that the aes is smaller in *Nfib*$^{-/-}$ hindbrains (A'). Ventral views of (B,B') E14, (C,C') E15, (D,D') E16, (E,E') E17, and (F,F') E18 hindbrains show time course of PN development in *Nfib*$^{+/-}$ and *Nfib*$^{-/-}$ hindbrains. Ventral views are oriented with rostral pointing up (R in panel B). Arrowheads indicate the ventral midline. Scale bars = 500 μm in A' (for A,A'); 250 μm for B,B'–F,F'.

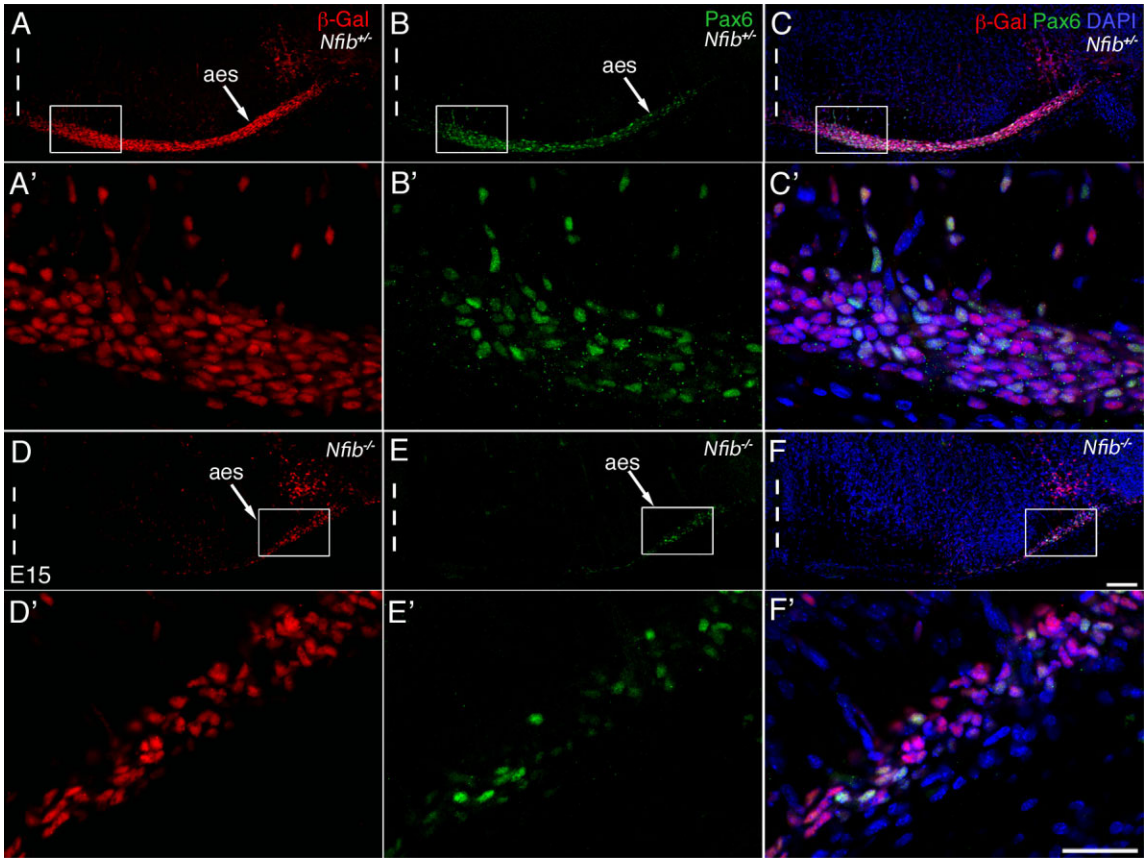

Figure 7.
Overlapping expression of β-gal and Pax6 in the aes. **A–F:** Double immunostaining with (A,D) anti-β-gal (red) and (B,E) anti-Pax6 (green) antibodies on coronal sections of E15 (A–C) *Nfib*$^{+/-}$ and (D–F) *Nfib*$^{-/-}$ mice. C,F: Overlays of β-gal and Pax6 staining, with sections counterstained for cell nuclei with DAPI (blue). **A'-F':** Higher magnifications of the boxed regions in A–F, respectively. Both β-gal and Pax6 are expressed in the aes, with virtually all Pax6+ cells expressing β-gal. As assessed using either marker, the aes has not progressed as far in *Nfib*$^{-/-}$ hindbrain when compared to *Nfib*$^{+/-}$ hindbrain. Scale bars = 100 μm in F (for A–F); 50 μm in F' (for A'–F').

press Math1, Pax6, and Barhl1 (Engelkamp et al., 1999; Li et al., 2004; Machold and Fishell, 2005; Wang et al., 2005).

The mossy fiber-specific pattern of precerebellar NFI-B expression is consistent with lineage studies demonstrating that the hindbrain mossy fiber nuclei are derived from a pool of progenitors distinct from those giving rise to the inferior olive. While the LRL in its entirety can be defined by expression of the transcription factor *Pax6*, the progenitors within the LRL are compartmentalized. A more dorsal subdomain expresses Math1 and high levels of Wnt1 and gives rise to mossy fiber neurons, while a more ventral subdomain expresses Neurogenin1 and low levels of Wnt1 and gives rise to climbing fiber neurons (Rodriguez and Dymecki, 2000; Landsberg et al., 2005; Machold and Fishell, 2005; Wang et al., 2005; Nichols and Bruce, 2006). As early as E12, NFI-B expression is particularly high in the LRL, and encompasses the entire Pax6-positive domain. Although this domain includes the Neurogenin1-positive domain that gives rise to climbing fiber neurons, NFI-B (like Pax6) is not expressed in the inferior olive. Therefore, based on its expression pattern, we would not expect NFI-B to parcellate the rhombic lip in a manner akin to Wnt1 and Math1, although we cannot rule out a potential function for NFI-B in regulating progenitor identity in a manner similar to that suggested for Pax6 (Landsberg et al., 2005).

The expression of NFI proteins in a subset of hindbrain nuclei is consistent with other studies of NFI expression. During development, members of the NFI family are expressed in different patterns throughout the body (Chaudhry et al., 1997). Within the brain, NFI family members are found in subsets of neurons and glia. For instance, NFI-A and NFI-B are expressed in laterally projecting neurons of the cerebral cortex, but are largely excluded from callosally projecting neurons (Plachez et al., 2008). NFI expression has also been observed in hippocampus and other regions of the telencephalon and diencephalon, and in granule neurons of the cerebellum (Wang et al., 2007; Plachez et al., 2008). Our results here combined with these earlier studies suggest that NFI proteins may play a role in generating and maintaining the identity of specific populations of neurons.

NFI family members are also expressed in glial populations, including those in the spinal cord as well as the midline glia of the forebrain (Shu et al., 2003; Deneen et al., 2006; Plachez et al., 2008). The expression observed here in the precerebellar migratory streams and nuclei is neuronal, as glial markers are

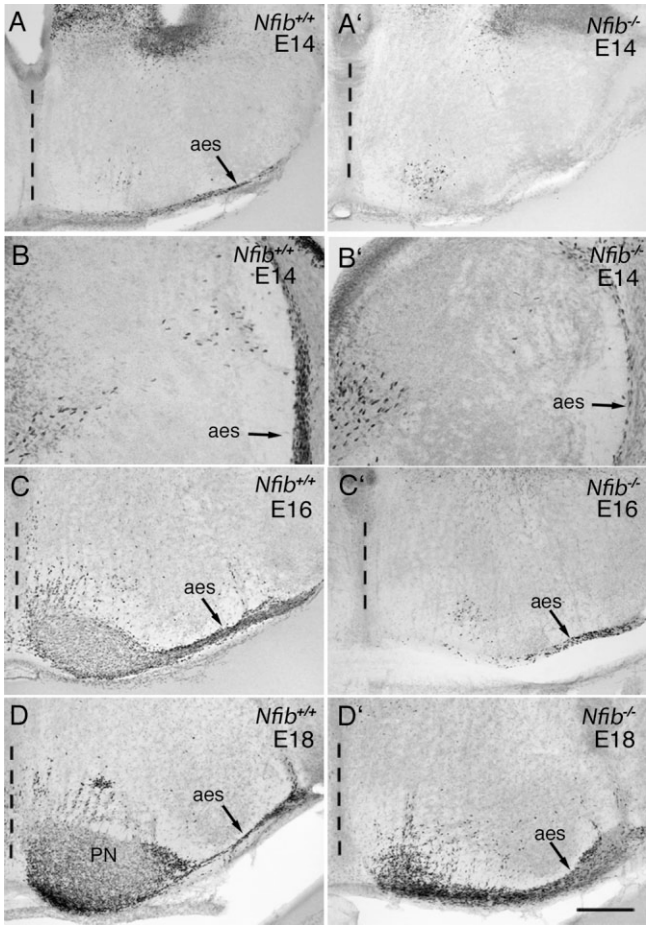

Figure 8.
Analysis of Pax6 expression in *Nfib*$^{-/-}$ hindbrains is consistent with a delay in PN development. **A,A':** Pax6 immunostaining on coronal sections of E14 (A) *Nfib*$^{+/-}$ and (A') *Nfib*$^{-/-}$ mice demonstrates the absence of the aes in the ventrolateral *Nfib*$^{-/-}$ hindbrain. **B,B':** Pax6 immunostaining on coronal sections of E14 (B) *Nfib*$^{+/-}$ and (B') *Nfib*$^{-/-}$ mice (sections are caudal to those in A,A') demonstrates the presence of the aes earlier in its migration (more proximal to the LRL compared to the position depicted in A,A'). **C,C':** Pax6 immunostaining on coronal sections of E16 (C) *Nfib*$^{+/-}$ and (C') *Nfib*$^{-/-}$ mice. The aes is present in *Nfib*$^{-/-}$ hindbrain, but has not reached the ventral midline. **D,D':** Pax6 immunostaining on coronal sections of E18 (D) *Nfib*$^{+/-}$ and (D') *Nfib*$^{-/-}$ mice. In *Nfib*$^{-/-}$ hindbrain, the aes is larger than at earlier ages. In addition, the PN has begun to form, although it is significantly smaller than in controls. Dashed lines in all panels indicate the midline. Scale bar = 250μm in D' (for A–B'); 500 μm for C–D'.

not expressed by cells in the aes (Yee et al., 1999), and GFAP-positive astrocytes are not found within the perinatal PN (Bastmeyer et al., 1998). We cannot rule out a later expression in astrocytes, nor the possibility of glial expression in other mid- and hindbrain nuclei studied here.

NFI-B function in precerebellar development

The expression of NFI-B in precerebellar mossy fiber neurons at all phases of their development is consistent with functional roles in regulating multiple developmental processes, including neurogenesis, cell migration, and axon outgrowth or other aspects of neuronal differentiation. Previous loss of function studies show that NFI proteins are required for proper development of neuronal and glial populations in the cerebral cortex, hippocampus, cerebellum, and spinal cord (das Neves et al., 1999; Shu et al., 2003; Steele-Perkins et al., 2005; Deneen et al., 2006; Driller et al., 2007; Wang et al., 2007; Campbell et al., 2008). Interestingly, different developmental processes appear to be affected in different areas of the brain, suggesting NFI family members have context-dependent functions, and therefore operate differently depending on the cell type in which they are expressed.

Consistent with its proposed role in pontine development, we had previously reported that the PN was severely reduced in E18 *Nfib*$^{-/-}$ mice (Steele-Perkins et al., 2005). The data presented here demonstrate that this reduction is due at least in part to a significant delay in PN development, with pontine neurons entering the aes, reaching the ventral midline, and invading the hindbrain parenchyma substantially later than in control animals. Such a delay necessarily results in a PN that is smaller than that found in control littermates at any given embryonic age. There are a number of possible causes for this phenotype, including a delay in neurogenesis or a slowing of cell migration. In the former case, pontine neurons would be produced later than usual, but then migrate normally. In general, such a role might be expected given the well-known role of NFI factors in regulating DNA replication as well as transcription (Gronostajski, 2000). In addition, NFI proteins have been shown to regulate specific populations of precursor cells in spinal cord and lung (Grunder et al., 2002; Steele-Perkins et al., 2005; Deneen et al., 2006), and *Nfix* knockout mice show accumulation of Pax6-positive cells, representing putative progenitor cells, in the lateral telencephalic ventricles (Campbell et al., 2008). Our finding that significantly fewer pontine neurons are generated at E13 in the absence of *Nfib* further supports a role for this transcription factor in the regulation of neurogenesis. Such a role would also account for a reduction in the size of the PN, although further experiments are required to confirm if this is also the cause of the delay in pontine development.

Many transcription factors regulate cell migration and axon outgrowth. More specifically, *Pax6, Barhl1, Nscl1/2*, and both *Hoxa2* and *Hoxb2* regulate various steps of pontine neuron migration (Engelkamp et al., 1999; Li et al., 2004; Schmid et al., 2007; Geisen et al. 2008). It is therefore possible that, in addition to reduced neurogenesis, the delay in pontine development may also result from a slowing of pontine neuron migration. Indeed, NFI proteins regulate the migration of cells in the cerebellum, forebrain, and spinal cord (Shu et al., 2003; Deneen et al., 2006; Wang et al., 2007). In addition, NFI proteins control the expression of factors that can regulate the rate of cell migration. One such factor, N-cadherin (Wang et al., 2007), has been shown to regulate the migration of precerebellar neurons (Taniguchi et al., 2006). While a decrease in migration speed could result in the observed developmental delay, our data do not support the idea that the guidance of migration is regulated by *Nfib*. First, the targeting of migrating pontine neurons appears normal, as they form an anatomically normal aes and appear to leave the aes at the correct site. Second, the *Nfib*$^{-/-}$ pontine phenotype is distinct from those observed after loss of other genes that are known to regulate the directionality of pontine neuron migration, such as netrin1 and DCC (Yee et al., 1999; Alcantara et al., 2000).

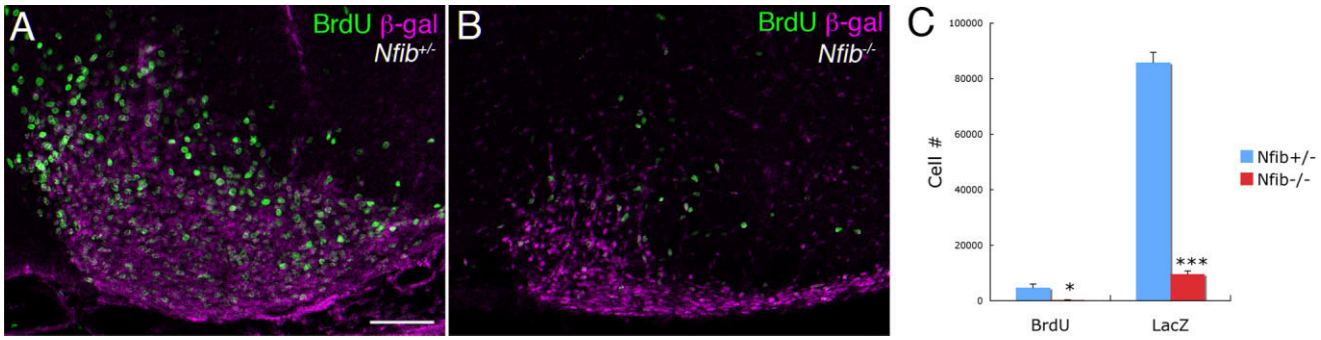

Figure 9.
Reduction of pontine neurogenesis in E13 Nfib knockout mice. **A,B:** Coronal sections of (A) *Nfib*$^{+/-}$ and (B) *Nfib*$^{-/-}$ hindbrain labeled at E13 with BrdU, immunostained for BrdU (green) and β-gal (magenta). Fewer β-gal+ and BrdU+ cells are observed in the knockout. **C:** Total number of BrdU+ and β-gal+ cells in *Nfib*$^{+/-}$ and *Nfib*$^{-/-}$ hindbrains. There is an approximately 90% reduction of cell number in both cases (exact numbers are listed in Results). *$P < 0.05$, ***$P < 0.001$ (unpaired *t*-test). Scale bar = 100 μm in A (for A,B).

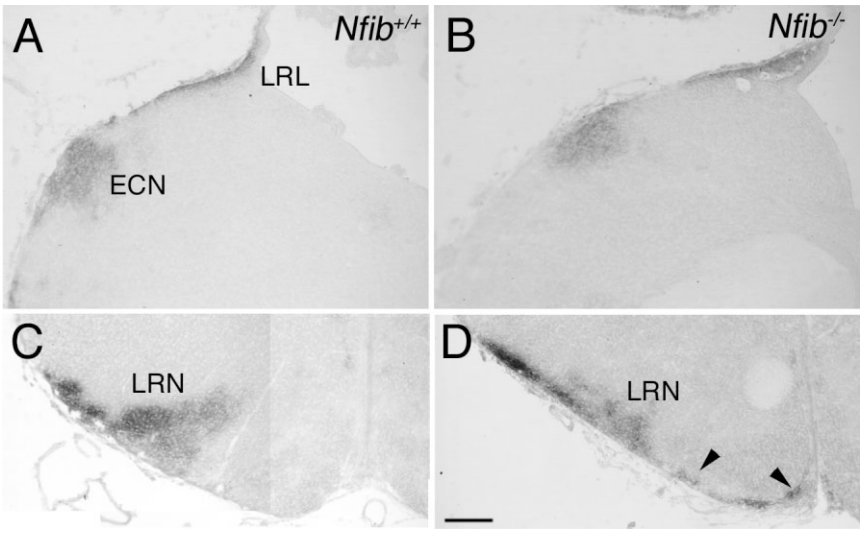

Figure 10.
Formation of the LRN and ECN in *Nfib* knockout mice. In situ hybridization for *Barhl1* in E18 **(A,C)** *Nfib*$^{+/+}$ and **(B,D)** *Nfib*$^{-/-}$ mice. In both cases, expression can be seen in migrating cells that have just departed the LRL, and the ECN and LRN can be identified. Ectopic *Barhl1* expression is observed in the *Nfib*$^{-/-}$ hindbrain adjacent to the ventral midline (arrow in D). Scale bars = 200 μm in D (for A–D).

Regulation of LRN and ECN development by *Nfib*

Neurons of the LRN and ECN, like those of the PN, arise from the LRL. Also like the PN, these more caudal populations exhibit a developmental delay in the absence of *Nfib*. However, there are two unique aspects of the development of the caudal populations. First, unlike the PN, a grossly normal ECN and a significant albeit misshapen LRN is present. This may indicate a less severe caudal phenotype in the *Nfib* mutant. Alternatively, this may reflect the earlier development of the caudal populations. As the *Nfib* knockout is perinatal lethal, the posterior populations may have largely completed development despite the delay, whereas the PN has not sufficient time to catch up. It will be necessary to develop a conditional *Nfib* knockout to address this issue.

The second unique aspect of the posterior *Nfib* phenotype is the presence of ectopic cells stretching from the LRN to the medial edge of the IO. It is unlikely that these cells represent LRN neurons that have been respecified to a climbing fiber identity (e.g., Landsberg et al., 2005), as these neurons still express the *Barhl1*, a mossy fiber marker. Another possibility is that the ectopic cells represent a population of LRN neurons that have mistargeted during cell migration. Interestingly, knockdown of N-cadherin slows the migration of LRN and ECN neurons, and this slowing leads to a failure of midline crossing (Taniguchi et al., 2006). Instead, cells target the anatomically correct location on the ipsilateral side, perhaps because the environment of the migrating neurons changes during the longer migration period. The late generation of LRN neurons or a slowing of their migration in the *Nfib*$^{-/-}$ mouse could create a similar situation in which a subset of developing cells fail to migrate across the ventral midline due to the presence of an older, less permissive environment. As NFI factors have been shown to regulate N-cadherin expression in the cer-

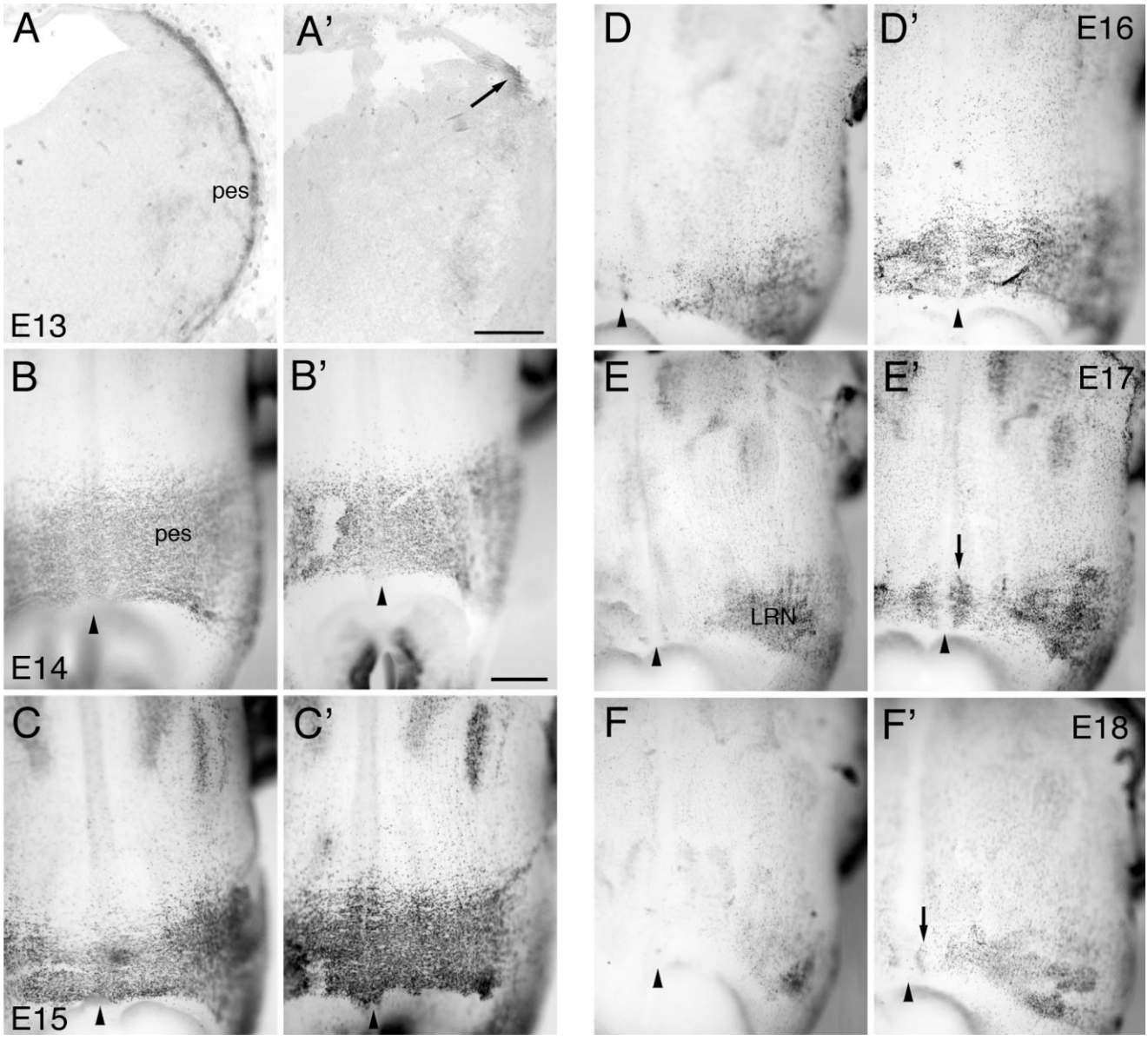

Figure 11.
Developmental delay of posterior mossy fiber populations in *Nfib* knockout mice. **A,A':** In situ hybridization for *Barhl1* on coronal sections of E13 (A) *Nfib*$^{+/+}$ and (A') *Nfib*$^{-/-}$ hindbrain. *Barhl1* expression in the mutant (arrow in A') is seen only in the vicinity of the LRL, and does not extend ventrally. **B,B'–F,F':** Immunostaining for β-gal in whole-mount preparations of (B,B') E14, (C,C') E15, (D,D') E16, (E,E') E17, and (F,F') E18 hindbrains from (B–F) *Nfib*$^{+/-}$ and (B'–F') *Nfib*$^{-/-}$ mice. All views are of the ventral surface, with the rostral end at the top of each panel; arrowheads indicate the position of the ventral midline. At E14 and E15 (B,B',C,C'), both controls and mutants have β-gal+ cells populating the pes on the ventral surface. Controls at E16 and later ages have a well-defined LRN (D–F), whereas E16 mutants still have many cells populating the pes in the vicinity of the ventral midline (D'). In E17 and E18 mutants, although the LRN is present, β-gal+ cells persist adjacent to the ventral midline (arrows in E',F') and appear to be continuous with the LRN. Scale bars = 200 μm in A' (for A,A'); 625 μm in B' (for B,B',C,C') and 500 μm (for D–F,D'–F').

ebellum (Wang et al., 2007), one possible explanation of the phenotype observed here would be a loss of N-cadherin expression in the absence of *Nfib*, leading to a slowing of migration.

Functional interactions of NFI transcription factors

The coexpression of multiple NFI proteins in the developing PN raises the question of whether these transcription factors act with some specificity, or whether they act redundantly to regulate the development or function of the structures in which they are expressed. While NFI proteins bind to the same DNA target sequences with similar affinities, they can differentially activate at least some promoters (Chaudhry et al., 1998; Mukhopadhyay et al., 2001), suggesting a mechanism for specific NFI action. Such differences may be due to differences in the C-terminal transactivation domain of individual

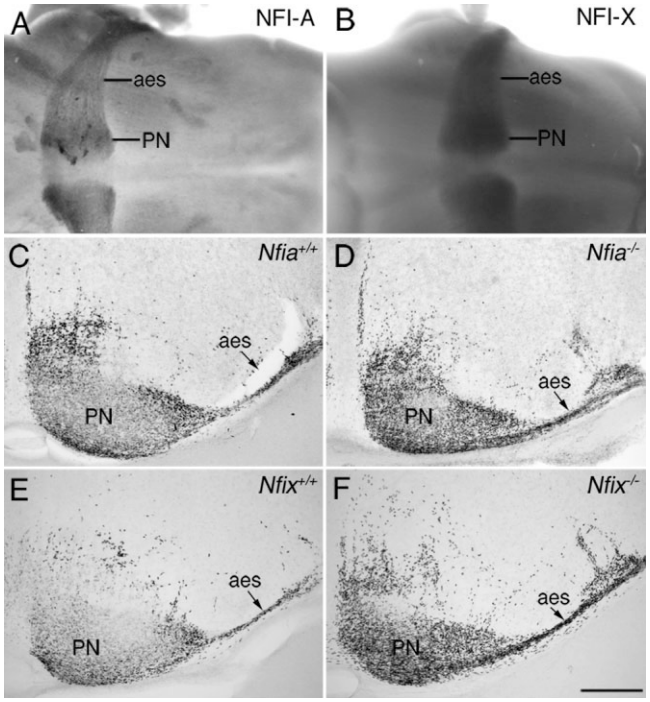

Figure 12.
The PN is apparently normal in both *Nfia* and *Nfix* knockout mice. **A:** Ventral view of an E16 hindbrain immunostained for NFI-A, showing expression in the aes and PN. **B:** Ventral view of an E16 hindbrain hybridized to an *Nfix* antisense RNA probe, showing *Nfix* mRNA in the aes and PN. Rostral is to the left in A and B. **C–F:** Pax6 immunoreactivity on coronal sections of E18 (C) $Nfia^{+/+}$, (D) $Nfia^{-/-}$, (E) $Nfix^{+/+}$, and (F) $Nfix^{-/-}$ mice. The aes and PN appear normal in both $Nfia^{-/-}$ and $Nfix^{-/-}$ mice. Scale bar in F= 200 μm for A,B; 500 μm for C–F.

family members. Furthermore, NFI protein function requires that they form either heterodimers or homodimers (Kruse and Sippel, 1994; Chaudhry et al., 1998). Thus, when NFI proteins are coexpressed, heterodimer formation may be one mechanism by which individual family members cooperate to coregulate specific steps in development. The overall action of NFI proteins in a given cell or tissue may depend on the levels of each individual NFI protein expressed, the activity of those proteins on target promoters, and the relative ability of each factor to form homodimers and heterodimers.

The overlapping expression of NFI factors in the PN (Figs. 4, 12; Chaudhry et al., 1997; Gesemann et al., 2001) suggests that they may cooperate in directing pontine development. We observe here, however, that the $Nfib^{-/-}$ PN exhibits a drastic reduction at E18.5, while $Nfia^{-/-}$ and $Nfix^{-/-}$ PN appear to be largely unchanged. This situation is distinct from that in the forebrain, where both *Nfia* and *Nfib* mutants exhibit agenesis of the corpus callosum, loss of the hippocampal commissure, and a loss of midline glia, although the *Nfib* cortical phenotype is more severe (das Neves et al., 1999; Shu et al., 2003; Steele-Perkins et al., 2005). *Nfix* knockouts do not exhibit callosal agenesis but instead uniquely possess ectopic Pax6-positive and doublecortin-positive cells within the lateral ventricles (Campbell et al., 2008; although an independent line has been reported with a different phenotype: Driller et al., 2007). Phenotypes in other organs, such as the lung, are also associated with only one of the NFI family members.

The phenotypic differences observed in the different *Nfi* lines may be a reflection of different levels of protein expression of individual NFI family members, which are as yet unknown, or differences in transcriptional activation potential. Alternatively, the differences in pontine phenotype may reflect true differences in downstream targets of individual NFI factors. Identification of such downstream genes will shed light on the degree to which individual NFI family members function with specificity.

ACKNOWLEDGMENTS

We thank Chad Bernardelli, Kimberly Valentino, and Faith Scipio for the genotyping and breeding of animals, Rebecca Pacifico and Katie Burke for technical assistance, and Mengqing Xiang for the gift of the *Barhl1* probe. We also thank Adam Puche for help and advice, and Reha Erzurumlu for comments on the article. The 4D7 monoclonal antibody developed by M. Yamamoto was obtained from the Developmental Studies Hybridoma Bank developed under the auspices of the NICHD and maintained by the University of Iowa, Department of Biological Sciences, Iowa City, Iowa.

LITERATURE CITED

Adams AD, Choate DM, Thompson MA. 1995. NF1-L is the DNA-binding component of the protein complex at the peripherin negative regulatory element. J Biol Chem 270:6975–6983.

Alcantara S, Ruiz M, De Castro F, Soriano E, Sotelo C. 2000. Netrin 1 acts as an attractive or as a repulsive cue for distinct migrating neurons during the development of the cerebellar system. Development 127: 1359–1372.

Altman J, Bayer S. 1997. Development of the cerebellar system in relation to its evolution, structure, and functions. Petralia P, editor. Boca Raton, FL: CRC Press.

Backer S, Sakurai T, Grumet M, Sotelo C, Bloch-Gallego E. 2002. Nr-CAM and TAG-1 are expressed in distinct populations of developing precerebellar and cerebellar neurons. Neuroscience 113:743–748.

Bastmeyer M, Daston MM, Possel H, O'Leary DD. 1998. Collateral branch formation related to cellular structures in the axon tract during corticopontine target recognition. J Comp Neurol 392:1–18.

Baumeister H, Gronostajski RM, Lyons GE, Margolis FL. 1999. Identification of NFI-binding sites and cloning of NFI-cDNAs suggest a regulatory role for NFI transcription factors in olfactory neuron gene expression. Brain Res Mol Brain Res 72:65–79.

Bedford FK, Julius D, Ingraham HA. 1998. Neuronal expression of the 5HT3 serotonin receptor gene requires nuclear factor 1 complexes. J Neurosci 18:6186–6194.

Bourrat F, Sotelo C. 1988. Migratory pathways and neuritic differentiation of inferior olivary neurons in the rat embryo. Axonal tracing study using the in vitro slab technique. Brain Res 467:19–37.

Bourrat F, Sotelo C. 1990. Migratory pathways and selective aggregation of the lateral reticular neurons in the rat embryo: a horseradish peroxidase in vitro study, with special reference to migration patterns of the precerebellar nuclei. J Comp Neurol 294:1–13.

Campbell CE, Piper M, Plachez C, Yeh Y-T, Baizer JS, Osinski JM, Litwack ED, Richards LJ, Gronostajski RM. 2008. The transcription factor *Nfix* is essential for normal brain development. BMC Dev Biol 8:52.

Causeret F, Danne F, Ezan F, Sotelo C, Bloch-Gallego E. 2002. Slit antagonizes netrin-1 attractive effects during the migration of inferior olivary neurons. Dev Biol 246:429–440.

Chaudhry AZ, Lyons GE, Gronostajski RM. 1997. Expression patterns of the four nuclear factor I genes during mouse embryogenesis indicate a potential role in development. Dev Dyn 208:313–325.

Chaudhry AZ, Vitullo AD, Gronostajski RM. 1998. Nuclear factor I (NFI) isoforms differentially activate simple versus complex NFI-responsive promoters. J Biol Chem 273:18538–18546.

das Neves L, Duchala CS, Tolentino-Silva F, Haxhiu MA, Colmenares C, Macklin WB, Campbell CE, Butz KG, Gronostajski RM. 1999. Disruption of the murine nuclear factor I-A gene (*Nfia*) results in perinatal

lethality, hydrocephalus, and agenesis of the corpus callosum. Proc Natl Acad Sci U S A 96:11946–11951.

Davis JA, Reed RR. 1996. Role of Olf-1 and Pax-6 transcription factors in neurodevelopment. J Neurosci 16:5082–5094.

Deneen B, Ho R, Lukaszewicz A, Hochstim CJ, Gronostajski RM, Anderson DJ. 2006. The transcription factor NFIA controls the onset of gliogenesis in the developing spinal cord. Neuron 52:953–968.

Di Meglio T, Nguyen-Ba-Charvet KT, Tessier-Lavigne M, Sotelo C, Chedotal A. 2008. Molecular mechanisms controlling midline crossing by precerebellar neurons. J Neurosci 28:6285–6294.

Dodd J, Morton SB, Karagogeos D, Yamamoto M, Jessell TM. 1988. Spatial regulation of axonal glycoprotein expression on subsets of embryonic spinal neurons. Neuron 1:105–116.

Driller K, Pagenstecher A, Uhl M, Omran H, Berlis A, Gründer A, Sippel AE. 2007. Nuclear factor I X deficiency causes brain malformation and severe skeletal defects. Mol Cell Biol 27:3855–3867.

Elder GA, Liang Z, Snyder SE, Lazzarini RA. 1992. Multiple nuclear factors interact with the promoter of the human neurofilament M gene. Brain Res Mol Brain Res 15:99–107.

Engelkamp D, Rashbass P, Seawright A, van Heyningen V. 1999. Role of Pax6 in development of the cerebellar system. Development 126: 3585–3596.

Geisen MJ, Di Meglio T, Pasqualetti M, Ducret S, Brunet J-F, Chedotal A, Rijli FM. 2008. *Hox* paralog group 2 genes control the migration of pontine neurons through slit-robo signaling. PLoS Biol 6:1178–1194.

Gesemann M, Litwack ED, Yee KT, Christen U, O'Leary DD. 2001. Identification of candidate genes for controlling development of the basilar pons by differential display PCR. Mol Cell Neurosci 18:1–12.

Gronostajski RM. 2000. Roles of the NFI/CTF gene family in transcription and development. Gene 249:31–45.

Grunder A, Ebel TT, Mallo M, Schwarzkopf G, Shimizu T, Sippel AE, Schrewe H. 2002. Nuclear factor I-B (*Nfib*) deficient mice have severe lung hypoplasia. Mech Dev 112:69–77.

Howard CV, Reed MG. 2005. Unbiased stereology. New York: Garland Science/BIOS Scientific Publishers.

Jacobowitz DM, Abbott LC. 1998. Chemoarchitectonic atlas of the developing mouse brain. Boca Raton, FL: CRC Press.

Kawauchi D, Taniguchi H, Watanabe H, Saito T, Murakami F. 2006. Direct visualization of nucleogenesis by precerebellar neurons: involvement of ventricle-directed, radial fibre-associated migration. Development 133:1113–1123.

Kruse U, Sippel AE. 1994. Transcription factor nuclear factor I proteins form stable homo- and heterodimers. FEBS Lett 348:46–50.

Kyriakopoulou K, de Diego I, Wassef M, Karagogeos D. 2002. A combination of chain and neurophilic migration involving the adhesion molecule TAG-1 in the caudal medulla. Development 129:287–296.

Lakso M, Pichel JG, Gorman JR, Sauer B, Okamoto Y, Lee E, Alt FW, Westphal H. 1996. Efficient in vivo manipulation of mouse genomic sequences at the zygote stage. Proc Natl Acad Sci U S A 93:5860–5865.

Landsberg RL, Awatramani RB, Hunter NL, Farago AF, DiPietrantonio HJ, Rodriguez CI, Dymecki SM. 2005. Hindbrain rhombic lip is comprised of discrete progenitor populations allocated by Pax6. Neuron 48:933–947.

Li S, Qiu F, Xu A, Price SM, Xiang M. 2004. Barhl1 regulates migration and survival of cerebellar granule cells by controlling expression of the neurotrophin-3 gene. J Neurosci 24:3104–3114.

Litwack ED, Babey R, Buser R, Gesemann M, O'Leary DDM. 2004. Identification and characterization of two novel brain-derived immunoglobulin superfamily members with unique structural organization. Mol Cell Neurosci 25:263–274.

Litwack ED, Lee Y, Mallott JM. 2006. Absence of the basilar pons in mice lacking a functional *Large* glycosyltransferase gene suggests a defect in pontine neuron migration. Brain Res 1117:12–17.

Machold R, Fishell G. 2005. Math1 is expressed in temporally discrete pools of cerebellar rhombic-lip neural progenitors. Neuron 48:17–24.

Marillat V, Sabatier C, Failli V, Matsunaga E, Sotelo C, Tessier-Lavigne M, Chedotal A. 2004. The slit receptor Rig-1/Robo3 controls midline crossing by hindbrain precerebellar neurons and axons. Neuron 43: 69–79.

Miura M, Tamura T, Mikoshiba K. 1990. Cell-specific expression of the mouse glial fibrillary acidic protein gene: identification of the cis- and trans-acting promoter elements for astrocyte-specific expression. J Neurochem 55:1180–1188.

Mukhopadhyay SS, Wyszomierski SL, Gronostajski RM, Rosen JM. 2001. Differential interactions of specific nuclear factor I isoforms with the glucocorticoid receptor and STAT5 in the cooperative regulation of WAP gene transcription. Mol Cell Biol 21:6859–6869.

Nichols DH, Bruce LL. 2006. Migratory routes and fates of cells transcribing the Wnt-1 gene in the murine hindbrain. Dev Dyn 235:285–300.

Obst-Pernberg K, Medina L, Redies C. 2001. Expression of R-cadherin and N-cadherin by cell groups and fiber tracts in the developing mouse forebrain: relation to the formation of functional circuits. Neuroscience 106:505–533.

Okada T, Keino-Masu K, Masu M. 2007. Migration and nucleogenesis of mouse precerebellar neurons visualized by in utero electroporation of a green fluorescent protein gene. Neurosci Res 57:40–49.

Paxinos G, Franklin KB. 2001. The mouse brain in stereotaxic coordinates. San Diego: Academic Press.

Plachez C, Lindwall C, Sunn N, Piper M, Moldrich RX, Campbell CE, Osinski JM, Gronostajski RM, Richards LJ. 2008. Nuclear factor one gene expression in the developing forebrain. J Comp Neurol 508:385–401.

Rodriguez CI, Dymecki SM. 2000. Origin of the precerebellar system. Neuron 27:475–486.

Schmahmann JD, Ko R, MacMore J. 2004. The human basis pontis: motor syndromes and topographic organization. Brain 127:1269–1291.

Schmid T, Krüger M, Braun T. 2007. NSCL-1 and -2 control the formation of precerebellar nuclei by orchestrating the migration of neuronal precursor cells. J Neurochem 102:2061–2072.

Shu T, Butz KG, Plachez C, Gronostajski RM, Richards LJ. 2003. Abnormal development of forebrain midline glia and commissural projections in Nfia knock-out mice. J Neurosci 23:203–212.

Steele-Perkins G, Plachez C, Butz KG, Yang G, Bachurski CJ, Kinsman SL, Litwack ED, Richards LJ, Gronostajski RM. 2005. The transcription factor gene Nfib is essential for both lung maturation and brain development. Mol Cell Biol 25:685–698.

Stoykova A, Gruss P. 1994. Expression of *Pax*-genes in developing and adult brain as suggested by expression patterns. J Neurosci 14:1395–1412.

Taber Pierce E. 1966. Time of origin of neurons in the brain stem of the mouse. Histogenesis of the nuclei griseum pontis, corporis pontobulbaris and reticularis tegmenti pontis (Bechterew) in the mouse. An autoradiographic study. J Comp Neurol 129:219–254.

Taber Pierce E. 1973. Time of origin of neurons in the brain stem of the mouse. Prog Brain Res 40:53–65.

Tamura T, Miura M, Ikenaka K, Mikoshiba K. 1988. Analysis of transcription control elements of the mouse myelin basic protein gene in HeLa cell extracts: demonstration of a strong NFI-binding motif in the upstream region. Nucleic Acids Res 16:11441–11459.

Taniguchi H, Kawauchi D, Nishida K, Murakami F. 2006. Classic cadherins regulate tangential migration of precerebellar neurons in the caudal hindbrain. Development 133:1923–1931.

Wang W, Stock RE, Gronostajski RM, Wong YW, Schachner M, Kilpatrick DL. 2004. A role for nuclear factor I in the intrinsic control of cerebellar granule neuron gene expression. J Biol Chem 279:53491–53497.

Wang VY, Rose MF, Zoghbi HY. 2005. Math1 expression redefines the rhombic lip derivatives and reveals novel lineages within the brainstem and cerebellum. Neuron 48:31–43.

Wang W, Mullikin-Kilpatrick D, Crandall JE, Gronostajski RM, Litwack ED, Kilpatrick DL. 2007. Nuclear factor I coordinates multiple phases of cerebellar granule cell development via regulation of cell adhesion molecules. J Neurosci 27:6115–6127.

Wolfer DP, Henehan-Beatty A, Stoeckli ET, Sonderegger P, Lipp HP. 1994. Distribution of TAG-1/axonin-1 in fibre tracts and migratory streams of the developing mouse nervous system. J Comp Neurol 345:1–32.

Yamamoto M, Boyer AM, Crandall JE, Edwards M, Tanaka H. 1986. Distribution of stage-specific neurite-associated proteins in the developing murine nervous system recognized by a monoclonal antibody. J Neurosci 6:3576–3594.

Yee KT, Simon HH, Tessier-Lavigne M, O'Leary DM. 1999. Extension of long leading processes and neuronal migration in the mammalian brain directed by the chemoattractant netrin-1. Neuron 24:607–622.